Ultrasound and Microbubble-Targeted Delivery of Macromolecules Is Regulated by Induction of Endocytosis and Pore Formation

Bernadet D.M. Meijering, Lynda J.M. Juffermans, Annemieke van Wamel, Rob H. Henning, Inge S. Zuhorn, Marcia Emmer, Amanda M.G. Versteilen, Walter J. Paulus, Wiek H. van Gilst, Klazina Kooiman, Nico de Jong, René J.P. Musters, Leo E. Deelman and Otto Kamp

Circulation Research 2009, 104:679-687: originally published online January 22, 2009
doi: 10.1161/CIRCRESAHA.108.183806
Circulation Research is published by the American Heart Association. 7272 Greenville Avenue, Dallas, TX 72514
 Print ISSN: 0009-7330. Online ISSN: 1524-4571

Ultrasound and Microbubble-Targeted Delivery of Macromolecules Is Regulated by Induction of Endocytosis and Pore Formation

Bernadet D.M. Meijering,* Lynda J.M. Juffermans,* Annemieke van Wamel, Rob H. Henning, Inge S. Zuhorn, Marcia Emmer, Amanda M.G. Versteilen, Walter J. Paulus, Wiek H. van Gilst, Klazina Kooiman, Nico de Jong, René J.P. Musters, Leo E. Deelman, Otto Kamp

Abstract—Contrast microbubbles in combination with ultrasound (US) are promising vehicles for local drug and gene delivery. However, the exact mechanisms behind intracellular delivery of therapeutic compounds remain to be resolved. We hypothesized that endocytosis and pore formation are involved during US and microbubble targeted delivery (UMTD) of therapeutic compounds. Therefore, primary endothelial cells were subjected to UMTD of fluorescent dextrans (4.4 to 500 kDa) using 1 MHz pulsed US with 0.22-MPa peak-negative pressure, during 30 seconds. Fluorescence microscopy showed homogeneous distribution of 4.4- and 70-kDa dextrans through the cytosol, and localization of 155- and 500-kDa dextrans in distinct vesicles after UMTD. After ATP depletion, reduced uptake of 4.4-kDa dextran and no uptake of 500-kDa dextran was observed after UMTD. Independently inhibiting clathrin- and caveolae-mediated endocytosis, as well as macropinocytosis significantly decreased intracellular delivery of 4.4- to 500-kDa dextrans. Furthermore, 3D fluorescence microscopy demonstrated dextran vesicles (500 kDa) to colocalize with caveolin-1 and especially clathrin. Finally, after UMTD of dextran (500 kDa) into rat femoral artery endothelium in vivo, dextran molecules were again localized in vesicles that partially colocalized with caveolin-1 and clathrin. Together, these data indicated uptake of molecules via endocytosis after UMTD. In addition to triggering endocytosis, UMTD also evoked transient pore formation, as demonstrated by the influx of calcium ions and cellular release of preloaded dextrans after US and microbubble exposure. In conclusion, these data demonstrate that endocytosis is a key mechanism in UMTD besides transient pore formation, with the contribution of endocytosis being dependent on molecular size. **(*Circ Res*. 2009;104:679-687.)**

Key Words: ultrasound microbubble targeted delivery ■ cell membrane pore ■ endocytosis ■ dextran ■ endothelial cells

Conventional delivery methods for drugs or genes, such as systemic administration via intravenous injection or oral administration, often do not suffice for therapeutic compounds such as peptides, silencing RNAs and genes.[1] A recent development in delivery systems for therapeutic compounds is the microbubble–ultrasound (US) interaction.[2,3] Before its use as a clinical modality, it is of utmost importance to obtain new physiological insights into the mechanisms of uptake by US and microbubble-exposed cells.

Microbubbles were originally developed as US contrast agents and are administered intravenously to the systemic circulation to enhance scattering of blood in echocardiography. They consist of a gas core stabilized with an encapsulation, ranging from 1 to 10 μm in diameter.[4] Nowadays, research focuses on the use of US and microbubbles for therapeutic applications. It has been demonstrated that US-exposed microbubbles can achieve safe and efficient local delivery of a variety of drugs[5,6] and genes.[7–9] In an US field, microbubbles will oscillate, and this may stimulate cells to admit the drug or gene.[10] The advantage of using US and microbubbles is that only the microbubbles in the US beam will be activated. In this way, delivery can be targeted to specific organs or sites by focusing the US beam on the specific target. This is indicated by the term US microbubble-targeted delivery (UMTD).

Original received July 23, 2008; revision received December 20, 2008; accepted January 13, 2009.

From the Department of Clinical Pharmacology (B.D.M.M., R.H.H., W.H.v.G., L.E.D.), University Medical Center Groningen, University of Groningen; Departments of Cardiology and Physiology (L.J.M.J., A.M.G.V., W.J.P., R.J.P.M., O.K.), VU University Medical Center, Amsterdam; Department of Biomedical Engineering (A.v.W., M.E., K.K., N.d.J.), Thorax Center, Erasmus MC, Rotterdam; Interuniversity Cardiology Institute of the Netherlands (B.D.M.M., L.J.M.J., A.v.W., W.H.v.G., N.d.J., L.E.D., O.K.), Utrecht; and Department of Cell Biology/Membrane Cell Biology (I.S.Z.), University Medical Center Groningen, University of Groningen, The Netherlands.

*Both authors contributed equally to this study.

Correspondence to Lynda J.M. Juffermans, VU University Medical Center, Department of Physiology, Room C170, Van der Boechorststraat 7, 1081 BT Amsterdam, The Netherlands. E-mail ljm.juffermans@vumc.nl

Circulation Research **is available at http://circres.ahajournals.org** **DOI: 10.1161/CIRCRESAHA.108.183806**

However, the exact mechanism of cellular uptake of therapeutics after UMTD is not fully understood. One of the principal mechanisms is thought to be induction of cell membrane pores.[11,12] Studies using scanning-electron microscopy revealed pore-like structures in the cell membrane after treatment by US either with or without microbubbles.[1,8,11,13] The presence of enhanced transmembrane ion fluxes during US and microbubble exposure was also demonstrated.[14,15] Although the hypothesis of pore formation during UMTD is supported by these studies, it was recently questioned in studies by Duvshani-Eshet and colleagues.[16,17] In these studies, pore-like structures were found in both US and microbubble-exposed cells, as well as in control cells.[16] Furthermore, atomic-force microscopy studies suggested that these pore-like structures represented depressions in the membrane rather than actual pores. Exposing cells to US and microbubbles altered both diameter and depth of these depressions,[17] indicating that the depressions in the membrane might represent endocytotic invaginations. Interestingly, Juffermans et al recently demonstrated that US-exposed microbubbles induced formation of hydrogen peroxide (H_2O_2) and an influx of calcium ions, causing local hyperpolarization of the cell membrane.[11,18] In addition, other studies demonstrated that H_2O_2 and a rise in intracellular calcium levels are directly correlated with endocytosis.[19–21]

Nevertheless, because there is still no consensus about the internalization mechanisms involved in UMTD, the aim of this study was to examine whether macromolecules enter the cell solely via transient pores, or that endocytosis might also be involved in the uptake during UMTD. As a model for drug delivery, uptake of dextrans ranging from 4.4 to 500-kDa in size was studied. Primary endothelial cells and rat femoral artery endothelium, the prime target cells for intravenous microbubbles, were subjected to UMTD of differentially sized dextran molecules to study whether the mechanism behind UMTD is dependent on molecular size.

Materials and Methods

Cell Culture

Primary bovine aortic endothelial cells (BAECs) (Cell Applications, San Diego, Calif) were cultured as described previously.[22] Cells between passage 3 and 7 were used for UMTD experiments. Forty-eight hours before UMTD, cells were seeded at 33% confluence to 1 of the 2 gas-permeable, US-transparent membranes of an Opticell cell culture chamber (Biocrystal, Westerville, Ohio).

Ultrasound Exposure

Before UMTD, the Opticell chamber was mounted in the experimental acoustic setup, described in detail elsewhere[22] and, in brief, in the online data supplement, available at http://circres.ahajournals.org. Cells were exposed to sine-wave US-bursts with a 6.2% duty cycle and a 20-Hz pulse repetition frequency for 30 seconds. Peak negative acoustic pressure generated at the region of interest was 0.22 MPa, as verified with a calibrated hydrophone (PVDFZ44-0400, Specialty Engineering Associates, Soquel, Calif).

Preparation of Microbubbles and Dextran Suspensions

The ultrasound contrast agent Sonovue (Bracco, High Wycombe, UK) was reconstituted in 5 mL of saline solution according to the protocol of the manufacturer, resulting in a preparation containing 2 to 5×10^8 microbubbles per milliliter. Tetramethylrhodamine isothiocyanate–labeled dextran (4.4, 70, or 155-kDa; Sigma-Aldrich), fluorescein isothiocyanate (FITC)-labeled dextran (500-kDa; Sigma-Aldrich), or lysine-fixable FITC-labeled dextran (500-kDa, Molecular Probes, Invitrogen) was added to 125 μL of Sonovue, with a final concentration of 2 mg/mL in 10 mL PBS.

Cellular Distribution

Above described microbubble–dextran solution was added to the cells directly followed by the US protocol. Immediately after UMTD, cells were washed with PBS at room temperature and confocal laser microscopy images were taken with a $\times$100 oil-immersion lens (Carl Zeiss, Sliedrecht, The Netherlands) to investigate the cellular distribution and localization of the dextran.

Inhibition of Endocytosis During UMTD

To prevent active uptake of extracellular molecules, cells were depleted from ATP, as described in detail in the online data supplement. Cells were preincubated with ATP-depletion buffer or with PBS for 30 minutes, followed by the UMTD protocol. To study the involvement of different endocytosis pathways, cells were pretreated 30 minutes with chlorpromazine (15 μmol/L; Sigma-Aldrich), inhibitor of clathrin-mediated endocytosis; filipin (4 μg/mL; Sigma-Aldrich), inhibitor of caveolin-mediated endocytosis; or wortmannin (0.1 μmol/L; Sigma-Aldrich), inhibitor of macropinocytosis before UMTD of 4.4-, 70-, 155-, and 500-kDa dextrans. The specificity of the inhibitor was tested in a separate assay, as described in the online data supplement. Confocal images were acquired directly following UMTD using a $\times$40 oil-immersion lens (Carl-Zeiss).

Immunostaining for Clathrin and Caveolin-1

Directly following UMTD of lysine-fixable FITC-labeled dextran (500-kDa), regions of interest were cut out the Opticell ($\approx$1.5 cm^2) and placed in PBS. Cells were fixated and stained with antibodies for clathrin and caveolin-1, as described in detail in the online data supplement. Clathrin and caveolin-1 are established markers for clathrin-mediated and caveolin-mediated endocytosis, respectively. No appropriate marker for macropinocytosis is available.

In Vivo Dextran Delivery

The animal study was approved by the Animal Research Committee at the VU University Medical Center. Both femoral arteries of Wistar rats (n=4) were cannulated and infused with microbubble–dextran (500 kDa, FITC-labeled, lysine-fixable) solution, followed by US exposure on the left femoral artery. Both arteries were dissected and stained with antibodies for clathrin and caveolin-1 for detection of colocalization with dextran. The experimental protocol is described in detail in the online data supplement.

US and Microbubble-Induced Pore Formation

To study pore formation, the influx of calcium ions was measured with the fluorescent probe Fluo-4 (Molecular Probes), a cell-permeant acetoxymethyl ester sensitive for free cytosolic calcium. To acquire time-lapse images during US exposure the transducer was mounted on the microscope, as described elsewhere.[15] To study the effect of inhibitors of endocytosis on the US and microbubble-evoked calcium influx, cells were preincubated 30 minutes with chlorpromazine, filipin, and wortmannin at concentrations indicated above before the calcium measurements.

To further investigate pore formation, cells were preloaded with fluorescent dextrans using the syringe loading protocol of Clarke and McNeil,[23] with minor adaptations described in detail in the online data supplement. Cells were exposed to US and microbubble according to the UMTD protocol described above, with the exception that no dextran was incubated with the microbubbles. Immediately after US and microbubbles, confocal images were taken using a $\times$40 oil-immersion lens (Carl Zeiss), and dextran release was measured.

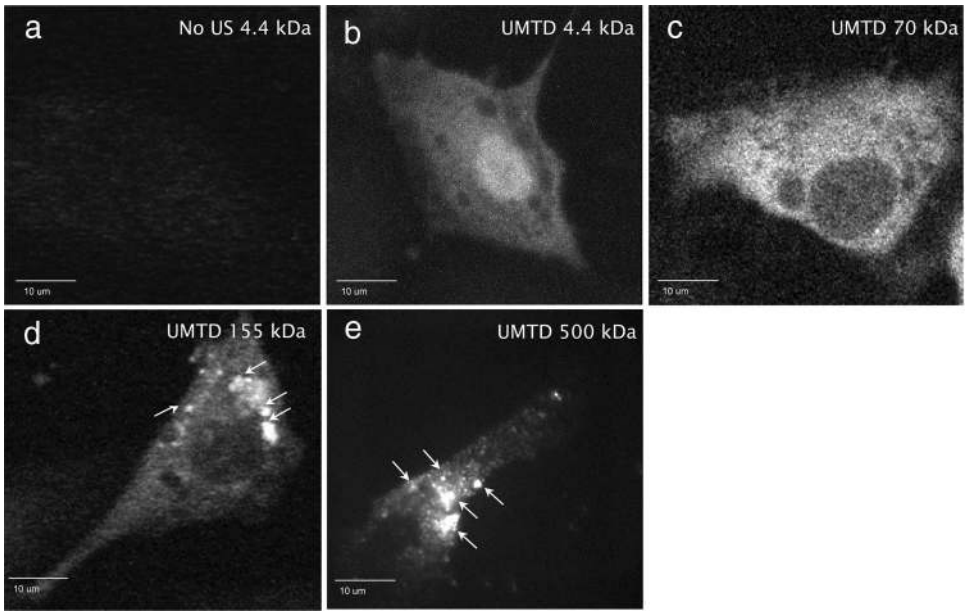

Figure 1. Cellular distribution of fluorescent dextrans after UMTD. a, No uptake of 4.4-kDa dextran in the absence of US. b, Homogeneous distribution in the cytosol, and nucleus of 4.4-kDa dextran after UMTD. c, Homogeneous distribution in the cytosol of 70-kDa dextran but absence of nuclear localization. d, Localization of 155 kDa mainly in vesicle-like structures (see arrows). e, Vesicular-like localization of 500-kDa dextran.

Statistics

Data are presented as means±SEM. All experiments were repeated at least 3 times. Per condition at least 6 microscopical fields were analyzed, containing approximately 10 to 20 cells per field. Groups were tested for normal distribution with one sample Kolmogorov–Smirnov test. Differences between groups were tested using a 1-way ANOVA with Bonferroni post hoc analysis or the nonparametric Kruskal–Wallis test with Dunn's post hoc test. Differences between groups in the experiment of calcium influx were tested using 2-way ANOVA with Bonferroni post hoc analysis. A probability value of less than 0.05 was considered statistically significant.

Results

Cellular Distribution of Differently Sized Dextrans

After UMTD dextran molecules of 4.4 kDa showed a homogeneous distribution throughout the cytosol as well as in the nucleus (Figure 1b). Dextran molecules of 70 kDa showed a similar distribution pattern in the cytosol but were absent in the nucleus (Figure 1c). Larger dextrans (155 and 500 kDa) showed a different cytosolic pattern of distribution after UMTD, because they were mainly found in vesicle-like structures but lacked nuclear localization (Figure 1d and 1e, respectively). In the absence of US, no uptake of dextran molecules was found (Figure 1a; results shown for 4.4 kDa).

Inhibition of Endocytosis During UMTD

To further investigate whether vesicle-like dextran-positive structures found after UMTD were endocytotic vesicles, UMTD of dextran was studied after overall inhibition of endocytosis through ATP depletion of the cells as well as inhibition of specific endocytotic pathways. Deprivation of cells from ATP resulted in inactivation of the endocytotic machinery, because these cells were no longer capable to actively internalize transferrin (Figure 2a through 2c) or 70-kDa dextran (Figure II in the online data supplement). Interestingly, UMTD of 4.4-kDa dextran was still successful after ATP depletion (Figure 2d through 2f). However, mean intensity of fluorescence (MIF)±SEM decreased by 62% (no depletion: 365.4±15.1; ATP depletion: 138.7±13.3; $P<0.001$). UMTD of 500-kDa dextran was completely inhibited when cells were ATP-depleted (Figure 2g through 2i).

Blocking macropinocytosis (wortmannin) or clathrin-mediated endocytosis (chlorpromazine) both caused a significant decrease in MIF after UMTD of all studied dextran sizes (Figure 3). Filipin, inhibiting caveolin-mediated endocytosis, caused a significant decrease in MIF after UMTD of dextrans of 155 and 500 kDa (Figure 3c and 3d) but not for 4.4- and 70-kDa dextrans (Figure 3a and 3b). The specificity and degree of inhibition was studied separately for each inhibitor and is described in supplemental Table I.

Colocalization of Endocytosis Markers and 500-kDa Dextran Molecules

To further substantiate the role of endocytosis, we investigated whether internalized 500-kDa dextran colocalizes with clathrin and/or caveolin-1, which are established markers for 2 main routes of endocytosis. Figure 4 shows clear colocalization of dextran with clathrin (Figure 4b and 4c) and to a minor extent with caveolin-1 (Figure 4d and 4e), as demonstrated by the yellow/orange color in the merged images of dextran (green) and clathrin/caveolin-1 (red). The extent of colocalization was determined using Pearson's correlation factor. A positive correlation was found for dextran with clathrin was 0.35±0.06 ($P<0.001$, compared to hypothetical value of 0.0), for dextran with caveolin 0.19±0.05 ($P<0.01$). As control, no correlation was found for DAPI (nuclei) with either Cy3 (0.01±0.01, $P=0.3$) or Cy5 channel (−0.01±0.02, $P=0.7$) (both secondary antibodies).

In Vivo Dextran Delivery

Results derived from in vivo experiments showed that dextran molecules of 500 kDa were localized in vesicle-like structures in the endothelium of the rat femoral artery after UMTD (Figure 5a and 5b). Morphology of the endothelium

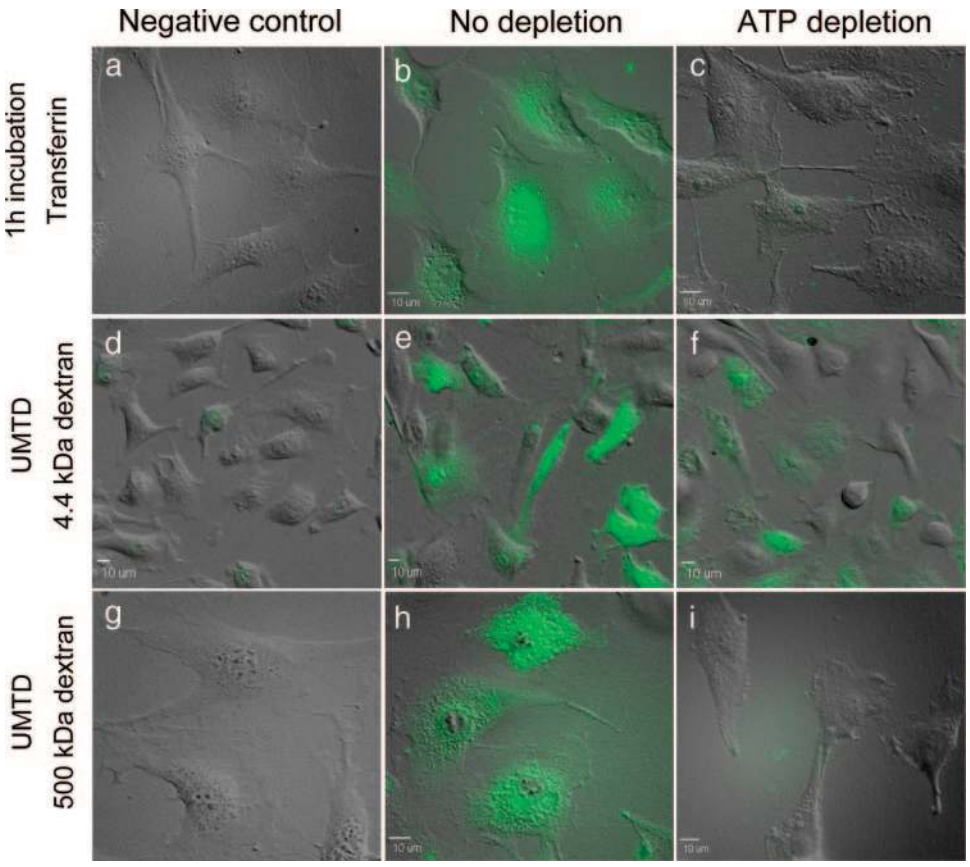

Figure 2. ATP depletion. Confocal images demonstrating uptake of transferrin and fluorescent dextrans (4.4 and 500 kDa) in the absence or presence of ATP depletion. Cells were pretreated with PBS (no depletion) or ATP-depletion buffer for 30 minutes. a, d, and g, Relative negative controls; no transferrin (a) and no UMTD (d and g). Uptake of transferrin after 1-hour incubation in PBS (c) and in ATP-depletion buffer (d). UMTD of 4.4-kDa dextran without depletion (e) and after ATP depletion (f). UMTD of 500-kDa dextran without depletion (g) and after ATP depletion (i).

and smooth muscle layer are shown in supplemental Figure III. A movie of the 3D stacked image is shown in the supplemental Movie file. No dextran was internalized in control artery not exposed to US. The endothelium was stained for clathrin and caveolin-1, and clear changes could be detected in the cellular pattern of both proteins in the US-exposed artery (Figure 5d and 5f) compared to control artery (Figure 5c and 5e). Furthermore, part of the dextran-positive vesicles clearly colocalized with clathrin (Figure 5d), indicated by the yellow/orange color. Colocalization with caveolin-1 was detected to a lesser degree (Figure 5f). After determining Pearson's correlation factor, results similar to the in vitro situation were found. A positive correlation factor of 0.35 ± 0.11 was found for clathrin, as well as for caveolin-1 (0.16 ± 0.04). Both correlations were significantly different from the hypothetical value of 0.0 ($P<0.05$). As control, no correlation was found for DAPI with either Cy3 (-0.05 ± 0.02, $P=0.7$) or Cy5 (-0.04 ± 0.02, $P=0.7$).

Ultrasound and Microbubble-Induced Pore Formation

Previously, we ascribed the increase in intracellular calcium levels after US and microbubbles exposure to transient pore formation in cardiomyoblast cells.[15] Also, US and microbubbles caused influx of calcium ions in BAECs. Fluorescent intensity reached a peak value of $186.4\pm3.4\%$, followed by a decrease toward basal levels (Figure 6a). There was no detectable change in the calcium influx in cells exposed to either US alone (no microbubbles) ($98.2\pm0.2\%$) or microbubbles alone (no US; $97.1\pm0.3\%$), or without both US and microbubbles ($94.3\pm0.3\%$, supplemental Figure IV). To investigate whether the inhibitors of endocytosis affected the calcium influx evoked by US and microbubbles, the calcium influx was also measured in the presence of chlorpromazine, filipin, and wortmannin. It was found that chlorpromazine and wortmannin did not significantly affect the US and microbubble-evoked influx (Figure 6b). However, filipin caused a large increase in the US and microbubble-evoked influx ($320.4\pm7.2\%$, $P<0.001$).

Furthermore, formation of transient pores was studied by cellular release of dextran following exposure to US and microbubbles (Figure 7). Cells were preloaded with dextran, and following US exposure MIF significantly decreased to $63.4\pm2.1\%$ for 4.4-kDa dextran (Figure 7a) and to $79.1\pm2.3\%$ for 155-kDa dextran (Figure 7b), compared to cells not exposed to US and microbubbles ($100.0\pm2.7\%$, $P<0.05$). Because filipin did not inhibit uptake of 4.4- and 70-kDa dextrans and augmented the US and microbubble-evoked calcium influx, its influence on dextran release was explored. Treatment with filipin alone, without US and microbubbles, did not cause a decrease in MIF ($100.0\pm1.5\%$, Figure 7). However, exposure of filipin-treated cells to US and microbubbles caused significantly more release of the 4.4-kDa dextrans ($54.9\pm3.1\%$, $P<0.05$), compared to non–filipin-treated cells exposed to US and microbubbles ($63.4\pm2.1\%$) (Figure 7a). Filipin-treatment of cells did not significantly alter the release of 155-kDa dextran ($75.6\pm2.3\%$) after US and microbubble exposure (Figure 7b).

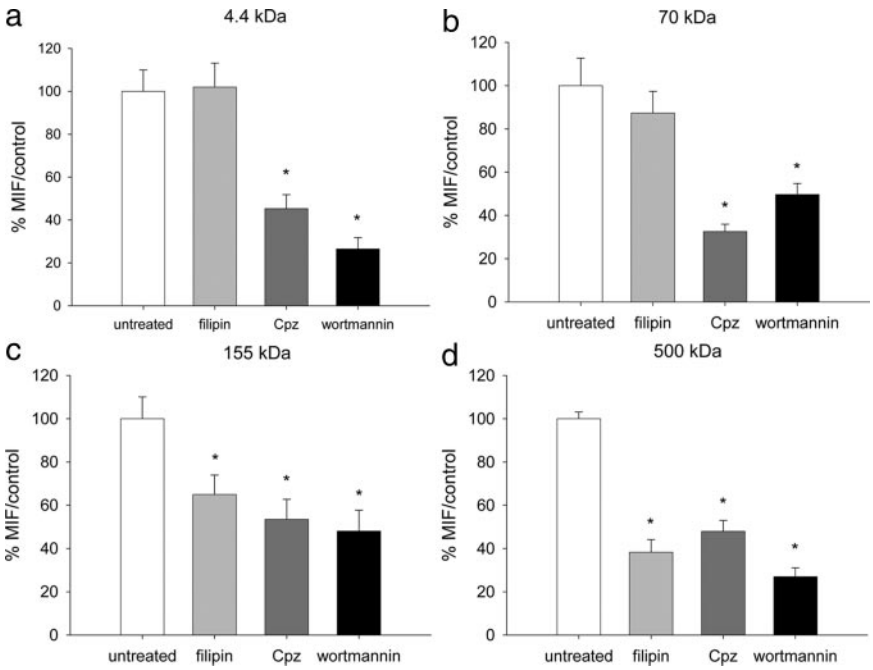

Figure 3. UMTD of dextrans in the presence of endocytosis blockers. Graphs show MIF±SEM for UMTD of all sizes of dextran, expressed as percentage of control (nonexposed cells). Significant reduction in cellular uptake of 4.4-kDa (a) and 70-kDa (b) dextrans in the presence of chlorpromazine (CPZ) (clathrin-mediated uptake) and wortmannin (macropinocytosis). Filipin (caveolin-mediated endocytosis) had no significant effect on the uptake of 4.4 and 70-kDa dextrans. Significant reduction in cellular uptake of 155-kDa (c) and 500-kDa (d) dextrans for all blockers.

Discussion

This is, to the best of our knowledge, the first study demonstrating that endocytosis plays a key role in UMTD of macromolecules sized between 4 and 500 kDa besides transient pores. The role of endocytosis was established by studying cellular localization of dextrans after UMTD, uptake of dextrans during ATP depletion, and the effect of individual blockers of the 3 main routes of endocytosis on dextran uptake. Furthermore, colocalization of 500-kDa dextran with markers for different endocytosis pathways was demonstrated in vitro as well as in vivo. In addition to endocytosis, we demonstrated the occurrence of transient pores in the cell membrane by showing both influx of calcium ions and cellular release of preloaded dextrans.

Studying cellular localization of fluorescent dextrans after UMTD, we found that the smaller dextran molecules of 4.4 and 70 kDa were homogeneously distributed throughout the cytosol. This is similar to the cellular distribution found after microinjection of dextran molecules from 3 to 70 kDa into the cytosol,[24,25] indicating that during UMTD the small dextran molecules enter cells via transient pores in the cell membrane. In contrast, dextran molecules of 155 and 500 kDa were mainly localized in vesicle-like structures after UMTD, indicating that the larger dextrans might be taken up via endocytosis.[26] When these dextran molecules had entered via pores, a homogeneous cytosolic distribution would be expected, comparable to the distribution of these dextran molecules after microinjection.[24,25] Therefore, uptake of

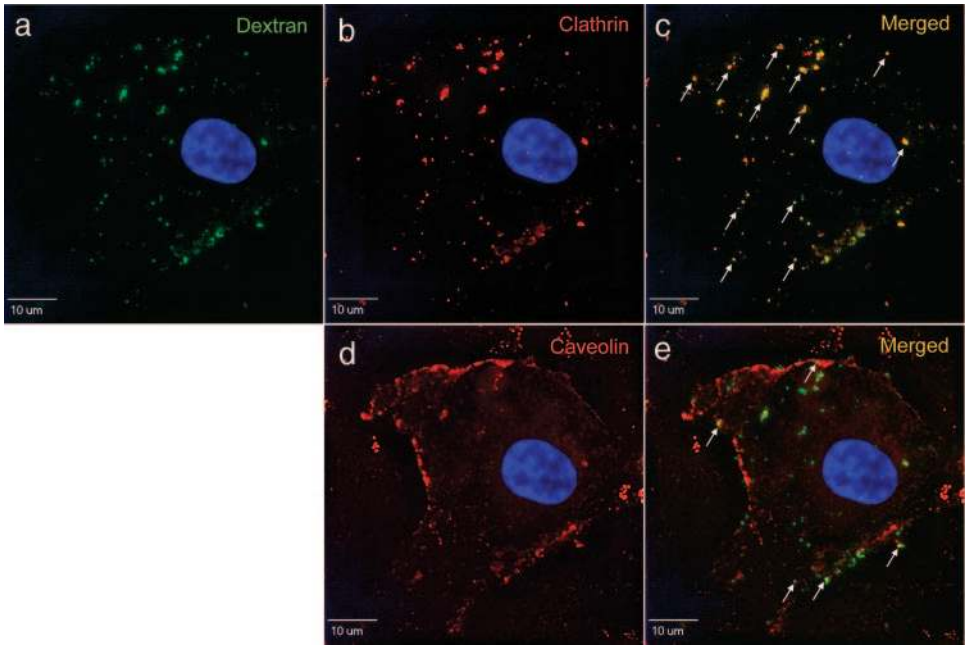

Figure 4. Colocalization of dextran with endocytosis markers after UMTD. One optical section from a 3D image stack is shown. a, Vesicle-like localization of 500-kDa dextran in green. b, Immunostaining for clathrin in red. c, Colocalization of dextran and clathrin, demonstrated by the yellow/orange color (indicated by arrows). d, Immunostaining for caveolin-1 in red. e, Colocalization of dextran and caveolin, demonstrated by the yellow/orange color (indicated by arrows). DAPI was used as nuclear counterstain.

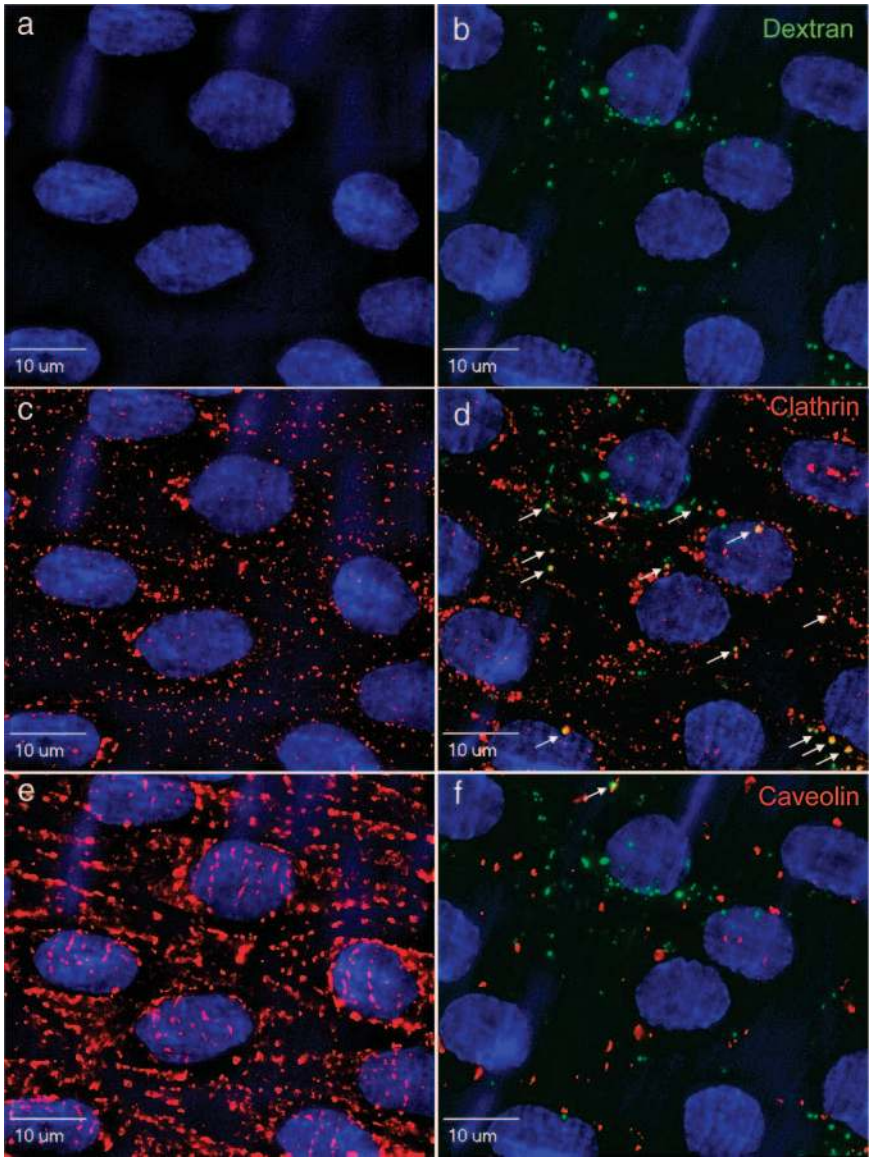

Figure 5. UMTD of 500-kDa dextran in vivo. Images are optical sections from 3D image stacks from the endothelial layer of the femoral arteries. a, c, and e, Image from control artery not exposed to US, demonstrating no dextran uptake. b, d, and f, Image from artery exposed to US, demonstrating dextran (green) uptake by the endothelium and localization in vesicle-like structures. c and d, Immunostaining for clathrin in red. Images demonstrate redistribution of clathrin-positive vesicles, indicated by more and larger clathrin-positive vesicles (possibly late endosomes) after UMTD. Arrows indicate colocalization of a part of the dextran-positive vesicles with clathrin. e and f, Immunostaining for caveolin-1 in red. Images demonstrate redistribution of caveolin-1, indicated by larger internalized caveolin-positive vesicles after UMTD, compared to a well-organized pattern on the cell membrane. However, minor colocalization with dextran is observed (a single arrow indicating yellow vesicle).

larger dextrans through UMTD appears to be mediated through other pathways than pore formation. After this first indication of endocytosis, these experiments were repeated while depriving the cell from ATP. Depleting the cells from ATP did not stop the 4.4 kDa from entering the cell but did significantly block the uptake by 62%. This decrease in fluorescence may be explained by either a 62% contribution of the endocytotic pathway or by a (partial) washout of the dextrans taken up via pores as these pores might not have resealed, because, like all cellular processes, this is also an energy-dependent process.[27] Interestingly, UMTD of 500-kDa dextran was completely blocked after ATP depletion, suggesting endocytosis as a route of entry during UMTD. Endocytosis is further evidenced as an important mechanism of UMTD by the decrease in cellular uptake of dextran molecules after inhibition of clathrin-mediated endocytosis, caveolin-mediated endocytosis, and macropinocytosis. Interestingly, not only the uptake of larger dextrans was inhibited by the endocytosis inhibitors but also the smaller dextrans showed a similar decrease after inhibiting clathrin-mediated endocytosis and macropinocytosis, although the confocal images of the smaller dextrans indicated uptake via pores. This discrepancy might be explained by the high level of fluorescence in the cytosol masking separate vesicles. Finally, colocalization of 500-kDa dextran with clathrin, and to a lesser degree caveolin-1, further supported the role of endocytosis during UMTD.

Importantly, the in vitro findings pointing to the involvement of endocytosis were extended to the in vivo situation. Using the same US parameters, 500-kDa dextrans were delivered into endothelium of the rat femoral artery. Confocal images of the US and microbubble-exposed artery showed conspicuous changes in the cellular pattern of caveolin-1 and clathrin, compared to the artery not exposed to US, indicating translocation of caveolin and clathrin on UMTD. It has been described in literature that in vitro for example shear stress can induce translocation of caveolin-1.[28,29] Furthermore, the dextran was clearly localized in vesicle-like structures that partially colocalized with both clathrin, and to a lesser degree caveolin-1, comparable to the in vitro data. These in vivo data

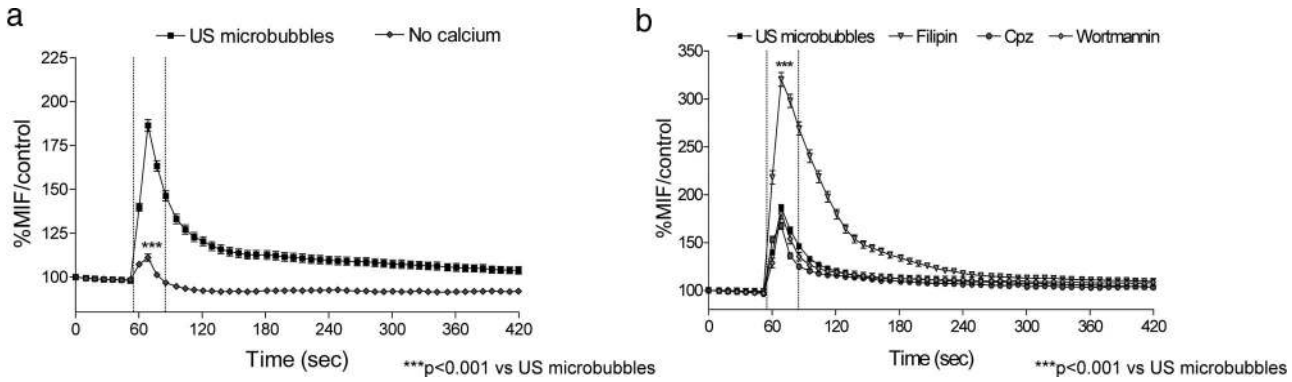

Figure 6. US- and microbubble-mediated calcium influx. Live-cell measurements of intracellular calcium levels over time. Data are shown as MIF±SEM, expressed as percentages of MIF on $t=0$ seconds. Dotted lines represent moments of US on and off switch, respectively. a, Increase in MIF during US-exposed microbubbles (black squares). The absence of extracellular calcium in the buffer resulted in a minor increase in fluorescence, compared to US and microbubbles with calcium ($P<0.001$). b, Effect of endocytosis inhibitors on the US- and microbubble-evoked calcium influx. Chlorpromazine and wortmannin have no significant effect on the US- and microbubble-evoked calcium influx; however, filipin significantly augmented the US and microbubble-evoked calcium influx ($P<0.001$).

further substantiated the role of endocytosis in UMTD of macromolecules to endothelial cells.

All 3 main routes of endocytosis were involved in UMTD of dextran molecules of 155 and 500 kDa, as demonstrated by the effect of the inhibitors of these routes of endocytosis. Caveolin-mediated endocytosis did not seem to be involved in UMTD of dextran molecules of 4.4 and 70 kDa, because filipin was not able to block the uptake of these smaller dextrans. However, it is known that filipin disrupts formation of caveolae by altering the distribution of cholesterol in the membrane,[30] thereby changing the physical properties of the membrane. This is confirmed by pretreating the cells with filipin, followed by exposure to US and microbubbles. Under these conditions, filipin enhanced the US and microbubble-induced calcium influx 3-fold. Secondly, filipin augmented the loss of cytosolic small fluorescent dextrans following UMTD but did not affect the loss of larger dextrans. Together, these data suggest that filipin increased vulnerability of the cell membrane and enhanced pore formation during exposure to US and microbubbles. Thus, caveolin-mediated endocytosis is also likely to play a role in UMTD of molecules ≤70 kDa. Unfortunately, replacing filipin with another inhibitor of caveolin-mediated endocytosis would most likely also result in increased formation of transient pores as these inhibitor all interfere with the physical properties of the cell membrane.[31]

We previously demonstrated the occurrence of transient pores evoked by US and microbubbles in cardiomyoblast cells. We showed that an increase in intracellular calcium was caused by the influx of calcium ions from the extracellular environment through transient pores in the cell membrane.[15] In the present study, it was found that also in BAECs, US and microbubbles evoked a calcium influx. Pore formation caused by US and microbubbles is further supported by the cellular release of fluorescent dextrans. Cells preloaded with 4.4-kDa dextran (diameter of 2.8 nm) showed a decrease in cytosolic fluorescence down to 63.4% after UMTD compared to only a small decrease down to 79.1% for 155-kDa dextran (diameter of 17 nm). This indicates that the contribution of transient pores is less important for UMTD of macromolecules ≥155 kDa using our US parameters. These data are in contrast with the study of Mehier-Humbert et al who suggested that dextran molecules with a diameter between 11.6 and 37.0 nm were able to enter the cell via pores, and no differences were found between molecule sizes.[13] However, the role of endocytosis in cellular entry of these molecules was not excluded in that study.

It remains unclear how UMTD induces endocytosis. It has been demonstrated that US-exposed microbubbles may cause a rise in temperature, which might affect membrane permeability and endocytosis. However, the rise in temperature has only been demonstrated for cavitating microbubbles.[32] Ex-

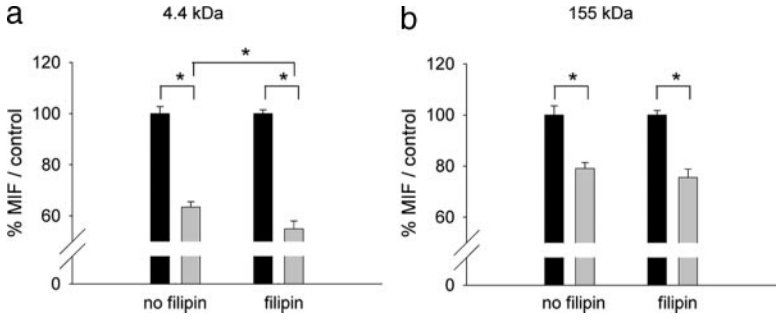

Figure 7. US- and microbubble-mediated cellular dextran release. a, MIF±SEM of 4.4-kDa dextran–loaded cells after US and microbubble exposure (gray bars), compared to cells not treated with US and microbubbles (black bars). US-exposed microbubbles resulted in a significant release of dextran ($P<0.05$). Pretreatment of cells with filipin before US and microbubble exposure resulted in significantly more dextran release ($P<0.05$), compared to cells that only received pretreatment with filipin (without US and microbubbles) and to cells exposed to US and microbubbles (no filipin). b, 155-kDa dextran–loaded cells. Exposure of cells to US and microbubbles (gray bars) resulted in a significant release of dextran ($P<0.05$), compared to cells not treated with US and microbubbles (black bars). Filipin had no additional effect on release of 155-kDa dextran. Release of 4.4-kDa dextran was significantly higher than release of 155-kDa dextran after US and microbubble exposure ($P<0.05$).

posing microbubbles to US with our parameters does not cause inertial cavitation and most likely also no increase in temperature. Several studies demonstrated that shear stress induces endocytosis in endothelial cells.[33–35] Flow of extracellular fluid induced by oscillation of microbubbles in an US field may cause shear stress and subsequent activation of endocytotic pathways. Furthermore, US and microbubble-evoked generation of H_2O_2, as well as a rise in intracellular calcium levels, is involved in inducing endocytosis.[15,18–21,36] Another recent publication showed that resealing of pores in the cell membrane, induced by a bacterial toxin, requires calcium-dependent endocytosis to remove the pores from the plasma membrane. They also found that this calcium-dependent endocytosis is required in a similar way to repair lesions formed in mechanically porated cells,[37] which may be comparable with US and microbubble-porated cells. Besides US and microbubble-induced uptake via endocytosis, another route of uptake that has been proposed is fusion of microbubble shell components with the cell membrane, especially in the case of lipid microbubbles. However, fusion has not yet been demonstrated experimentally, only suggested.[4,38] Furthermore, if fusion does take place, it is to be expected that this will lead to a homogeneous distribution of the dextran in the cytosol. In this study, we found a vesicular localization of the larger dextrans and a key role for endocytosis, arguing against an important role for fusion.

To summarize, UMTD provides opportunities for new therapies because of its low toxicity, low immunogenicity, noninvasive nature, local application, and its cost-effectiveness. Another advantage over other targeted delivery systems for therapeutic compounds is that molecular imaging and therapeutic compound delivery can be performed simultaneously.[39] The finding that the contribution of endocytosis and pore formation to intracellular delivery and subsequent subcellular localization of the therapeutic compound is dependent on the molecular size, should be taken into account when designing new effective therapies using UMTD. Pharmaceutical chemical compounds are generally smaller than 4 kDa and may have their target in the cytosol or nucleus, because they are small enough to pass the nuclear pore. Proteins may range from 4 to 500 kDa. DNA, which needs to enter the nucleus for effective therapy, often exceeds 500 kDa and is likely to be trapped in endosomes. This compartmentalization of therapeutic compounds and, most importantly genes, may affect therapy efficiency and should be taken into consideration when measuring drug action following UMTD. On the other hand, because many crucial signaling events are known to occur in these endosomes,[40] the endocytotic mechanism could also be exploited for therapy.

In conclusion, endocytosis plays a key role in UMTD of molecules sized between 4 and 500 kDa besides transient pore formation. The contribution of transient pores as a mechanism of UMTD decreases, when molecule size increases. These findings provide important new insight in the mechanisms of UMTD and will lead to the rational design of new drug or gene therapies involving UMTD.

Sources of Funding

This study was funded by the Interuniversity Cardiology Institute of The Netherlands.

Disclosures

None.

References

1. Schlicher RK, Radhakrishna H, Tolentino TP, Apkarian RP, Zarnitsyn V, Prausnitz MR. Mechanism of intracellular delivery by acoustic cavitation. *Ultrasound Med Biol*. 2006;32:915–924.
2. Newman CM, and Bettinger T. Gene therapy progress and prospects: ultrasound for gene transfer. *Gene Ther*. 2007;14:465–475.
3. Mayer CR, and Bekeredjian R. Ultrasonic gene and drug delivery to the cardiovascular system. *Adv Drug Deliv Rev*. 2008;60:1177–1192.
4. Dijkmans PA, Juffermans LJM, Musters RJP, van Wamel A, ten Cate F, van Gilst W, Visser CA, de Jong N, Kamp O. Microbubbles and ultrasound: from diagnosis to therapy. *Eur J Echocardiogr*. 2004;5:245–256.
5. Unger EC, McCreery TP, Sweitzer RH, Caldwell VE, Wu Y. Acoustically active lipospheres containing paclitaxel: a new therapeutic ultrasound contrast agent. *Invest Radiol*. 1998;33:886–892.
6. Bekeredjian R, Chen S, Grayburn PA, Shohet RV. Augmentation of cardiac protein delivery using ultrasound targeted microbubble destruction. *Ultrasound Med Biol*. 2005;31:687–691.
7. Chen S, Ding JH, Bekeredjian R, Yang BZ, Shohet RV, Johnston SA, Hohmeier HE, Newgard CB, Grayburn PA. Efficient gene delivery to pancreatic islets with ultrasonic microbubble destruction technology. *Proc Nat Acad Sci U S A*. 2006;103:8469–8474.
8. Taniyama Y, Tachibana K, Hiraoka K, Namba T, Yamasaki K, Hashiya N, Aoki M, Ogihara T, Yasufumi K, Morishita R. Local delivery of plasmid DNA into rat carotid artery using ultrasound. *Circulation*. 2002; 105:1233–1239.
9. Leong-Poi H, Kuliszewski MA, Lekas M, Sibbald M, Teichert-Kuliszewska K, Klibanov AL, Stewart DJ, Lindner JR. Therapeutic arteriogenesis by ultrasound-mediated VEGF165 plasmid gene delivery to chronically ischemic skeletal muscle. *Circ Res*. 2007;101:295–303.
10. van Wamel A, Bouakaz A, Versluis M, de Jong N. Micromanipulation of endothelial cells: ultrasound-microbubbles-cell interaction. *Ultrasound Med Biol*. 2004;30:1255–1258.
11. Tachibana K, Uchida T, Ogawa K, Yamashita N, Tamura K. Induction of cell-membrane porosity by ultrasound. *Lancet*. 1999;353:1409.
12. van Wamel A, Kooiman K, Harteveld M, Emmer M, Ten Cate FJ, Versluis M, de Jong N. Vibrating microbubbles poking individual cells: Drug transfer into cells via sonoporation. *J Control Release*. 2006;112: 149–155.
13. Mehier-Humbert S, Bettinger T, Yan F, Guy RH. Plasma membrane poration induced by ultrasound exposure: implication for drug delivery. *J Control Release*. 2005;104:213–222.
14. Deng CX, Sieling F, Pan H, Cui J. Ultrasound-induced cell membrane porosity. *Ultrasound Med Biol*. 2004;30:519–526.
15. Juffermans LJ, Dijkmans PA, Musters RJ, Visser CA, Kamp O. Transient permeabilization of cell membranes by ultrasound-exposed microbubbles is related to formation of hydrogen peroxide. *Am J Physiol Heart Circ Physiol*. 2006;291:H1595–H1601.
16. Duvshani-Eshet M, Machluf M. Therapeutic ultrasound optimization for gene delivery: a key factor achieving nuclear DNA localization. *J Control Release*. 2005;108:513–528.
17. Duvshani-Eshet M, Baruch L, Kesselman E, Shimoni E, Machluf M. Therapeutic ultrasound-mediated DNA to cell and nucleus: bioeffects revealed by confocal and atomic force microscopy. *Gene Ther*. 2006;13:163–172.
18. Juffermans LJ, Kamp O, Dijkmans PA, Visser CA, Musters RJ. Low-intensity ultrasound-exposed microbubbles provoke local hyperpolarization of the cell membrane via activation of BK(Ca) channels. *Ultrasound Med Biol*. 2008;34:502–508.
19. Sundqvist T, Liu SM. Hydrogen peroxide stimulates endocytosis in cultured bovine aortic endothelial cells. *Acta Physiol Scand*. 1993;149: 127–131.
20. MacDonald PE, Eliasson L, Rorsman P. Calcium increases endocytotic vesicle size and accelerates membrane fission in insulin-secreting INS-1 cells. *J Cell Sci*. 2005;118:5911–5920.
21. Saliez J, Bouzin C, Rath G, Ghisdal P, Desjardins F, Rezzani R, Rodella LF, Vriens J, Nilius B, Feron O, Balligand JL, Dessy C. Role of caveolar compartmentation in endothelium-derived hyperpolarizing factor-mediated relaxation: Ca2+ signals and gap junction function are regulated by caveolin in endothelial cells. *Circulation*. 2008;117:1065–1074.
22. Meijering BD, Henning RH, van Gilst W, Gavrilovic I, van Wamel A, Deelman LE. Optimization of ultrasound and microbubbles targeted gene

delivery to cultured primary endothelial cells. *J Drug Target*. 2007;15:664–671.
23. Clarke MS, McNeil PL. Syringe loading introduces macromolecules into living mammalian cell cytosol. *J Cell Sci*. 1992;102(pt 3):533–541.
24. Perez-Terzic C, Gacy AM, Bortolon R, Dzeja PP, Puceat M, Jaconi M, Prendergast FG, Terzic A. Structural plasticity of the cardiac nuclear pore complex in response to regulators of nuclear import. *Circ Res*. 1999;84:1292–1301.
25. Seksek O, Biwersi J, Verkman AS. Translational diffusion of macromolecule-sized solutes in cytoplasm and nucleus. *J Cell Biol*. 1997;138:131–142.
26. Miller DL, Quddus J. Sonoporation of monolayer cells by diagnostic ultrasound activation of contrast-agent gas bodies. *Ultrasound Med Biol*. 2003;26:661–667.
27. Bement WM, Yu HY, Burkel BM, Vaughan EM, Clark AG. Rehabilitation and the single cell. *Curr Opin Cell Biol*. 2007;19:95–100.
28. Sun RJ, Muller S, Stoltz JF, Wang X. Shear stress induces caveolin-1 translocation in cultured endothelial cells. *Eur Biophys J*. 2002;30:605–611.
29. Fawzi-Grancher S, Sun RJ, Traore M, Stoltz JF, Muller S. Role of Ca2+ in the effects of shear stress and TNF-alpha on caveolin-1 expression. *Clin Hemorheol Microcirc*. 2005;33:253–261.
30. Orlandi PA, Fishman PH. Filipin-dependent inhibition of cholera toxin: evidence for toxin internalization and activation through caveolae-like domains. *J Cell Biol*. 1998;141:905–915.
31. Byfield FJ, Aranda-Espinoza H, Romanenko VG, Rothblat GH, Levitan I. Cholesterol depletion increases membrane stiffness of aortic endothelial cells. *Biophys J*. 2004;87:3336–3343.
32. Hilgenfeldt S, Lohse D, Zomack M. Sound scattering and localized heat deposition of pulse-driven microbubbles. *J Acoust Soc Am*. 2000;107:3530–3539.
33. Apodaca G. Modulation of membrane traffic by mechanical stimuli. *Am J Physiol Renal Physiol*. 2002;282:F179–F190.
34. Niwa K, Sakai J, Karino T, Aonuma H, Watanabe T, Ohyama T, Inanami O, Kuwabara M. Reactive oxygen species mediate shear stress-induced fluid-phase endocytosis in vascular endothelial cells. *Free Radic Res*. 2006;40:167–174.
35. van Bavel E. Effects of shear stress on endothelial cells: possible relevance for ultrasound applications. *Prog Biophys Mol Biol*. 2007;93:374–383.
36. Wu LG. Kinetic regulation of vesicle endocytosis at synapses. *Trends Neurosci*. 2004;27:548–554.
37. Idone V, Tam C, Goss JW, Toomre D, Pypaert M, Andrews NW. Repair of injured plasma membrane by rapid Ca2+-dependent endocytosis. *J Cell Biol*. 2008;180:905–914.
38. Hernot S, Klibanov AL. Microbubbles in ultrasound-triggered drug and gene delivery. *Adv Drug Deliv Rev*. 2008;60:1153–1166.
39. Schneider M. Molecular imaging and ultrasound-assisted drug delivery. *J Endourol*. 2008;22:795–802.
40. Xu Y, Buikema H, Van Gilst WH, Henning RH. Caveolae and endothelial dysfunction: filling the caves in cardiovascular disease. *Eur J Pharmacol*. 2008;585:256–260.